Semnan University

Mechanics of Advanced Composite Structures

journal homepage: http://MACS.journals.semnan.ac.ir

Nonlinear Magneto-Nonlocal Vibration Analysis of Coupled Piezoelectric Micro-Plates Reinforced with Agglomerated CNTs

S. Amir*, A.R. Vossough, H. Vossough, E. Arshid

Department of Solid Mechanics, Faculty of Mechanical Engineering, University of Kashan, Kashan, Iran

KEYWORDS

Coupled system
Agglomerated CNTs
DQM
Piezoelectric
Magnetic field

ABSTRACT

The aim of this article is to analyze nonlinear electro-magneto vibration of a double-piezoelectric composite microplate-system (DPCMPS) pursuant to the nonlocal piezoelasticity theory. The two microplates are assumed to be connected by an enclosing elastic medium, which is simulated by the Pasternak foundation. Both of piezoelectric composite microplates are made of poly-vinylidene fluoride (PVDF) reinforced by agglomerated carbon nanotubes (CNTs). The Mori-Tanaka model is employed to compute the mechanical properties of composite. Applying nonlinear strain-displacement relations and contemplating charge equation for coupling between electrical and mechanical fields, the motion equations are derived in consonance to the energy method and Hamilton's principle. These equations can't be solved analytically as a result of their nonlinear terms. Hence, the differential quadrature method (DQM) is employed to solve the governing differential equations for the case when all four ends are clamped supported and free electrical boundary conditions. The frequency ratio of DPCMPS is inspected for three typical vibrational states, namely, out-of-phase, in-phase and the case when one microplate is fixed in the DPCMPS. A detailed parametric study is conducted to scrutinize the influences of the small scale coefficient, stiffness of the internal elastic medium, the volume fraction of the CNTs, agglomeration and magnetic field. The results reveal that with increasing volume fraction of the CNTs, the frequency of the structure increases. This study might be beneficial for the design and smart control of nano/micro devices such as MEMS and NEMS.

1. Introduction

Nanocomposites hold the promise of advances that exceed those achieved in recent decades in composite materials. The nanostructure generated by a nanophase in the polymer matrix represents a radical alternative to the structure of conventional polymer composites. These complex hybrid materials integrate the predominant surfaces of nanoparticles and the polymeric structure into a novel nanostructure, which produces critical fabrication and interface implementations leading to extraordinary properties [1]. PVDF is an ideal piezoelectric matrix as a result of characteristics including flexibility in thermoplastic conversion techniques, excellent dimensional stability, abrasion and corrosion resistance, high strength, and capability of maintaining its mechanical properties at elevated temperature. Consequently, it has found multiple applications in nanocomposites in a wide range of industries including oil and gas, petrochemical, wire and cable, electronics, automotive, and construction. Boron nitride nanotubes (BNNTs) applied as the matrix reinforcers, apart from having high mechanical, electrical, and chemical properties, present more resistant to oxidation than other conventional nano reinforces such as carbon nanotubes (CNTs). Hence, they are applied for high-temperature applications [2-6]. Both PVDF and BNNT are smart materials since they have piezoelectric properties.

Piezoelectricity is a classical discipline traced to the original work of Jacques and Pierre Curie around 1880. This phenomenon describes the relations between mechanical strains on a solid and its resulting electrical behavior resulting from changes in the electric polarization. One can generate an electrical output from a solid resulting from mechanical strains or can create a mechanical distortion resulting from the application of an electrical perturbation [7].

* Corresponding author. Tel.: +98-31-55913433; Fax: +98-31-55913444.
E-mail address: samir@kashanu.ac.ir; saeid_amir27111@yahoo.com

DOI: 10.22075/MACS.2019.16632.1185
Received 2018-11-29; Received in revised form 2019-05-20; Accepted 2019-08-27

Piezoelectric materials have been applied to manufacture various sensors, conductors, actuators, etc. in fact, they have become one of the smart materials nowadays [8].

Regarding research development into the application of smart nanocomposite (which PVDF and BNNT are as matrix and reinforcer, respectively), Barzoki et al. [8] explored electro-thermo-mechanical torsional buckling of a piezoelectric polymeric cylindrical shell reinforced by DWBNNTs with an elastic core. They concluded that the higher the in-fill core, the higher is dimensionless critical torsional buckling load. In another research, Barzoki et al. [9] investigated nonlinear buckling response of embedded piezoelectric cylindrical shell reinforced with BNNT under electro-thermo-mechanical loadings applying harmonic differential quadrature method (HDQM). They discovered that the critical buckling load increases when the piezoelectric effect is considered. Ghorbanpour et al. [10] demonstrated nonlinear vibration and stability of a smart composite micro tube made of PVDF reinforced by BNNTs embedded in an elastic medium under electro-thermal loadings is inspected. They concluded that the stability of the system is strongly dependent on the imposed electric potential and the volume percent of BNNTs reinforcement.

In recent years, small scale effect in micro and nano applications of the beam, plate, and shell type structures has been utilized on the basis of nonlocal elasticity theory which was initiated in the papers of Eringen [11-13]. He regarded the stress state at a given point as a function of the strain states of all points in the body, while the local continuum mechanics assumes that the stress state at a given point depends uniquely on the strain state at the same point. Shen et al. [14] explored the nonlocal plate model for nonlinear vibration of single-layer graphene sheets (SLGS) in thermal environments. Their results revealed that with properly selected small scale parameters and material properties, the nonlocal plate model could provide a remarkably accurate prediction of the graphene sheet behavior under nonlinear vibration in the thermal environment. Pradhan and Kumar [15] reported vibration analysis of orthotropic graphene sheets applying nonlocal elasticity theory and DQM. Their results indicated that the nonlocal effect increases as size of graphene sheet are decreased. Amir [16] examined Orthotropic patterns of visco-Pasternak foundation in nonlocal vibration of orthotropic graphene sheet under thermo-magnetic fields based on new first-order shear deformation theory. The results indicate that the stability of single-layer graphene sheet is strongly dependent on applied magnetic field. Ghorbanpour et al. [17] investigated Pasternak foundation effect on the axial and torsional wave propagation in the embedded double-walled carbon nanotubes (DWCNTs) applying nonlocal elasticity cylindrical shell theory. They concluded that the frequencies are dependent on small scale coefficient and shear modulus of the elastic medium.

The mentioned studies above on the nanostructures are on the basis of the nonlocal elasticity theory, which is not proper for direct application in the piezoelectric materials. Recently, Eringen's nonlocal elasticity theory was extended by Zhou et al. [18-20] for the piezoelectric materials. In the nonlocal piezoelectric materials, the stress state and the electric displacement at a given point are, respectively, as a function of the strain state and electric potential of all points in the body. Ke et al. [21] employed a nonlocal piezoelasticity model to nonlinear vibration analyze of the piezoelectric nanobeams. They applied DQM to study the effects of nonlocal parameter, temperature change and the external electric voltage on the nonlinear frequency of the piezoelectric nanobeams. Sobhy and Zenkour [22] discussed the magnetic field effect on thermomechanical buckling and vibration of viscoelastic sandwich nanobeams with CNT reinforced face sheets on a viscoelastic substrate. Moreover, Differential quadrature method for vibration analysis of electro-rheological sandwich plate with CNT reinforced nanocomposite face sheets subjected to electric field examined by Ghorbanpour Arani et al. [23]. Furthermore, in small-scales, nonlinear dynamic buckling analysis of embedded micro cylindrical shells reinforced with agglomerated CNTs applying strain gradient theory was researched by Tohidi et al. [24].

With respect to developmental works on mechanical behavior analysis of nano and micro plates, it should be noted that none of the researches mentioned above have considered a coupled double-plate system. Herein, Murmu and Adhikari [25] analyzed vibration of the nonlocal double nanoplate- system (NDNPS). Their study highlighted that the small-scale effects considerably influence the transverse vibration of NDNPS. Also, they elucidated that the boost of the stiffness of coupling springs in the NDNPS reduces the small scale effects during the asynchronous modes of vibration. Moreover, buckling behavior of the NDNPS was investigated by Murmu et al. [26], who indicated that the nonlocal effects in the coupled system are higher within creasing values of the nonlocal parameter for the case of synchronous buckling modes than in the asynchronous buckling modes. Furthermore, their analytical results indicated that the increase of the stiffness of the coupling springs in the double-GS-system reduces the nonlocal effects during the asynchronous modes of buckling. Exact solution

for nonlocal vibration of double-orthotropic nanoplates embedded in elastic medium was reported by Pouresmaeeli et al. [27], who manifested that the frequency of double orthotropic nanoplates is always smaller than that of double isotropic nanoplates. The three papers [25-27] have contemplated the Winkler model for simulation of elastic medium between two nanoplates. In this simplified model, a proportional interaction between pressure and deflection of SLGS is assumed, which is demonstrated in the form of discrete and independent vertical springs. Whereas, Pasternak suggested taking into account not only the normal stresses but also the transverse shear deformation and continuity among the spring elements, and its subsequent applications for developing the model for buckling analysis, which proved to be more accurate than the Winkler model. Recently, analysis of the coupled system of double layered graphene sheets (CS-DLGSs) embedded in a visco-Pasternak foundation is manifested by Ghorbanpour Arani et al. [28] who indicated that the frequency ratio of the CS-DLGSs is more than the SLGS. To the best of our knowledge, none of the works in the literature have contemplated the nonlinear terms in the governing equations for a coupled system. This study aims to deliberated nonlinear terms for vibration analysis of a DPCMPS in which two microplates are connected by an enclosing Pasternak foundation.

None of the aforementioned studies [25-28] have considered smart coupled structures, while these structures may be applied in mechanical behavior control of coupled micro and nano structures. Recently, buckling analysis and smart control of SLGS using elastically coupled PVDF nanoplate using the nonlocal piezoelasticity were examined by Ghorbanpour et al. [29], who indicated that the imposed external voltage is an effective controlling parameter for buckling of the SLGS. Moreover, their results revealed that the effect of external voltage becomes more prominent at higher nonlocal parameter and shear modulus. But paper [29] is linear analysis, and just one of two plates is smart.

However, to date, no study was reported in the literature on the vibration of an elastically coupled DPCMPS. Motivated by these considerations, in order to ameliorate the optimum design of smart microstructure, the authors aim to investigate the electro-magneto nonlinear nonlocal vibration of an elastically coupled DPCMPS. Herein, the two PVDF microplates reinforced by agglomerated CNTs are coupled by an enclosing Pasternak foundation. deliberated the nonlinear strain-displacement relations and charge equation, the nonlinear governing equations are derived applying energy method and Hamilton's principle. Hence, the DQM is presented to solve the nonlinear governing equations and estimate the frequency. In the present study, the influences of nonlocal parameters, temperature gradient, elastic medium constants, agglomeration and volume fraction of CNTs and magnetic field in polymer have been taken into account.

2. Formulation

2.1. Nonlocal Piezoelasticity

Pursuant to the theory of nonlocal piezoelasticity, the stress tensor and the electric displacement at a reference point depend not only on the strain components and electric field components in the same position but on all other points of the body as well. The nonlocal constitutive behavior for the piezoelectric material can be computed as follows [21]:

$$\sigma_{ij}^{nl}(x)=\int_{v}\alpha(|x-x'|,\tau)\sigma_{ij}^{l}dV(x'),\qquad \forall x\in V \tag{1}$$

$$D_{k}^{nl}=\int_{v}\alpha(|x-x'|,\tau)D_{k}^{l}dV(x'),\qquad \forall x\in V \tag{2}$$

where σ_{ij}^{nl} and σ_{ij}^{l} are, respectively, the nonlocal stress tensor and local stress tensor, D_{k}^{nl} and D_{k}^{l} are the components of the nonlocal and local electric displacement. $\alpha(|x-x'|,\tau)$ is the nonlocal modulus. $|x-x'|$ is the Euclidean distance, and $\tau=e_0a/l$ is defined that l is the external characteristic length, e_0 denotes a constant appropriate to each material, and a is an internal characteristic length of the material. Consequently, e_0a is a constant parameter that is acquired with molecular dynamics, experimental results, experimental studies, and molecular structure mechanics. In order to gain a constitutive equation of the nonlocal elasticity can be written as [30]:

$$(1-\mu\nabla^2)\sigma_{ij}^{nl}=\sigma_{ij}^{l}, \tag{3}$$

where the parameter $\mu=(e_0a)^2$ denotes the small scale effect on the response of structures in nano/micro size and ∇^2 is the Laplacian operator in the above equation. Similarly, Eq. (2) can be written as [20]:

$$(1-\mu\nabla^2)D_{k}^{nl}=D_{k}^{l}, \tag{4}$$

2.2. Classical Plate Theory

Based on the classical plate theory (CPT), which satisfies Kirchhoff assumption, the displacement field is expressed as [31]:

$$\begin{aligned}u(x,y,z,t)&=u_0(x,y,t)-z\frac{\partial w_0}{\partial x},\\ v(x,y,z,t)&=v_0(x,y,t)-z\frac{\partial w_0}{\partial y},\\ w(x,y,z,t)&=w_0(x,y,t),\end{aligned} \tag{5}$$

where (u, v, w) denote the total displacements of a point along with the (x, y, z) coordinates and (u_0, v_0, w_0) are the displacements of points on the mid-plane. The von-Kármán nonlinear strains associated with the above displacement field can be expressed in the following form [32]:

$$\begin{aligned}
\varepsilon_{xx} &= \frac{\partial u}{\partial x}+\frac{1}{2}(\frac{\partial w}{\partial x})^2,\\
\varepsilon_{yy} &= \frac{\partial v}{\partial y}+\frac{1}{2}(\frac{\partial w}{\partial y})^2,\\
\varepsilon_{xz} &= \frac{1}{2}(\frac{\partial u}{\partial z}+\frac{\partial w}{\partial x}),\\
\varepsilon_{yz} &= \frac{1}{2}(\frac{\partial v}{\partial z}+\frac{\partial w}{\partial y}),\\
\varepsilon_{xy} &= \frac{1}{2}(\frac{\partial u}{\partial y}+\frac{\partial v}{\partial x}+\frac{\partial w}{\partial x}\frac{\partial w}{\partial y}),\\
\varepsilon_{zz} &= \frac{\partial w}{\partial z},
\end{aligned} \tag{6}$$

On the basis of the CPT, shear strains ε_{xz}, ε_{yz} are contemplated negligible. Hence, the strain equations in terms of the mid-plane displacements are derived by substituting the Eq. (5) into the Eq. (6) as follows:

$$\begin{Bmatrix}\varepsilon_{xx}\\ \varepsilon_{yy}\\ \gamma_{xy}\end{Bmatrix}=\begin{Bmatrix}\frac{\partial u_0}{\partial x}+\frac{1}{2}(\frac{\partial w_0}{\partial x})^2\\ \frac{\partial v_0}{\partial y}+\frac{1}{2}(\frac{\partial w_0}{\partial y})^2\\ \frac{\partial u_0}{\partial y}+\frac{\partial v_0}{\partial y}+\frac{\partial w_0}{\partial x}\frac{\partial w_0}{\partial y}\end{Bmatrix}+z\begin{Bmatrix}-\frac{\partial^2 w_0}{\partial x^2}\\ -\frac{\partial^2 w_0}{\partial y^2}\\ -2\frac{\partial^2 w_0}{\partial x\partial y}\end{Bmatrix}, \tag{7}$$

The strain components ε_{xx}, $\varepsilon_{yy,}$ and γ_{xy} at an arbitrary point of the sheet are related to the middle surface strains and curvatures tensor as follows:

$$\begin{Bmatrix}\varepsilon_{xx}\\ \varepsilon_{yy}\\ \gamma_{xy}\end{Bmatrix}=\begin{Bmatrix}\varepsilon^0_{xx}\\ \varepsilon^0_{yy}\\ \gamma^0_{xy}\end{Bmatrix}+z\begin{Bmatrix}\varepsilon^1_{xx}\\ \varepsilon^1_{yy}\\ \gamma^1_{xy}\end{Bmatrix}, \tag{8}$$

where (ε^0_{xx}, ε^0_{yy}, γ^0_{xy}) are components of the membrane strains (middle surface strains) tensor and (ε^1_{xx}, ε^1_{yy}, γ^1_{xy}) are components of the bending strain (curvature) tensor.

2.3. Modeling of the Problem

An elastically coupled DPCMPS having the length l, the width b, and the thickness h, assuming that $h \ll l, b$ [32], is illustrated in Fig. 1.

The origin of the Cartesian coordinate system is contemplated at one corner of the middle surface of the microplate. The x, y, and z axes are taken in conformity with the length, width, and thickness of the microplates, respectively. The two microplates are created of PVDF and reinforced by CNTs in x-direction so that both microplates are identical.

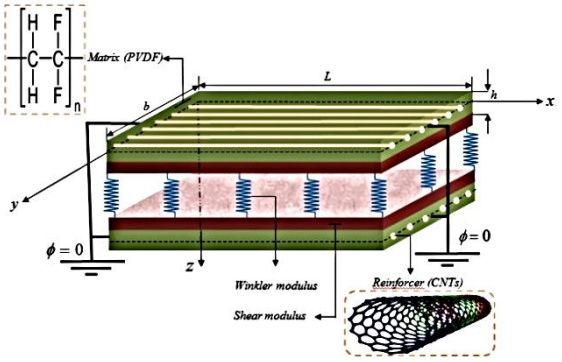

Fig. 1. Schematic of double-smart composite microplate-system.

The DPCMPS is subjected to uniform temperature change and polarized in x-direction. The two microplates are coupled by an elastic medium, which is simulated by the Pasternak foundation. As is well known this foundation model is characterized by two parameters: the Winkler constant k_w and shear constant k_g.

2.4. Constitutive Equations for Piezoelectric Materials

In a piezoelectric material, the application of an electric field to it will cause a strain proportional to the mechanical field strength, and vice versa. Pursuant to a piezoelectric microplate under electro-thermal loads, constitutive equations can be represented as [33]:

$$\begin{aligned}(1-\mu\nabla^2)\begin{bmatrix}\sigma^{nl}_{xx}\\ \sigma^{nl}_{yy}\\ \sigma^{nl}_{xy}\end{bmatrix}&=\begin{bmatrix}\bar{C}_{11} & \bar{C}_{12} & 0\\ \bar{C}_{21} & \bar{C}_{22} & 0\\ 0 & 0 & \bar{C}_{66}\end{bmatrix}\left(\begin{Bmatrix}\varepsilon_{xx}\\ \varepsilon_{yy}\\ \gamma_{xy}\end{Bmatrix}-\begin{pmatrix}\alpha_x\\ \alpha_y\\ 0\end{pmatrix}\Delta T\right)\\ &-\begin{bmatrix}e_{11} & 0 & 0\\ e_{12} & 0 & 0\\ 0 & e_{26} & 0\end{bmatrix}\begin{Bmatrix}E_{xx}\\ E_{yy}\\ E_{zz}\end{Bmatrix},\end{aligned} \tag{9}$$

$$\begin{aligned}(1-\mu\nabla^2)\begin{bmatrix}D^{nl}_{xx}\\ D^{nl}_{yy}\\ D^{nl}_{xy}\end{bmatrix}&=\begin{bmatrix}e_{11} & e_{12} & 0\\ 0 & 0 & e_{26}\\ 0 & 0 & 0\end{bmatrix}\left(\begin{Bmatrix}\varepsilon_{xx}\\ \varepsilon_{yy}\\ \gamma_{xy}\end{Bmatrix}-\begin{pmatrix}\alpha_x\\ \alpha_y\\ 0\end{pmatrix}\Delta T\right)\\ &-\begin{bmatrix}\epsilon_{11} & 0 & 0\\ 0 & \epsilon_{22} & 0\\ 0 & 0 & \epsilon_{22}\end{bmatrix}\begin{Bmatrix}E_{xx}\\ E_{yy}\\ E_{zz}\end{Bmatrix},\end{aligned} \tag{10}$$

where e_{ij}, ϵ_{ij} (i, j=1...,6), α_k (k=x, y), and ΔT are piezoelectric constants, dielectric constants, thermal expansion coefficients, and temperature gradient, respectively. C_{ij} is a component of stiffness tensor. Electric field tensor E can be written in term of electric potential ϕ as [34]:

$$E = -\nabla\phi. \tag{11}$$

2.5. Mori-Tanaka Approach

In this section, the effective modulus of the composite shell reinforced by CNTs is developed.

Different methods are available to estimate the overall properties of a composite [1]. As a result of its simplicity and accuracy, even at high volume fractions of the inclusions, the Mori-Tanaka method [1] is applied in this section. To begin with, the CNTs are assumed to be aligned and straight with the dispersion of uniform in the polymer. The matrix is assumed to be elastic and isotropic, with Young's modulus E_m and the Poisson's ratio ν_m. The constitutive relations for a layer of the composite with the principal axes parallel to the r, θ and z directions are [1]:

$$\begin{Bmatrix}\sigma_{11}\\ \sigma_{22}\\ \sigma_{33}\\ \sigma_{23}\\ \sigma_{13}\\ \sigma_{12}\end{Bmatrix}=\begin{bmatrix}k+m & l & k-m & 0 & 0 & 0\\ l & n & l & 0 & 0 & 0\\ k-m & l & k+m & 0 & 0 & 0\\ 0 & 0 & 0 & p & 0 & 0\\ 0 & 0 & 0 & 0 & m & 0\\ 0 & 0 & 0 & 0 & 0 & p\end{bmatrix}\begin{Bmatrix}\varepsilon_{11}\\ \varepsilon_{22}\\ \varepsilon_{33}\\ \gamma_{23}\\ \gamma_{13}\\ \gamma_{12}\end{Bmatrix} \tag{12}$$

where σ_{ij}, ε_{ij}, γ_{ij}, k, m, n, l, and p are the stress components, the strain components, and the stiffness coefficients, respectively. In consonance to the Mori-Tanaka method, the stiffness coefficients are shown by [1]:

$$k=\frac{E_m\{E_m c_m+2k_r(1+\nu_m)[1+c_r(1-2\nu_m)]\}}{2(1+\nu_m)[E_m(1+c_r-2\nu_m)+2c_m k_r(1-\nu_m-2\nu_m^2)]}$$

$$l=\frac{E_m\{c_m\nu_m[E_m+2k_r(1+\nu_m)]+2c_r l_r(1-\nu_m^2)]\}}{(1+\nu_m)[E_m(1+c_r-2\nu_m)+2c_m k_r(1-\nu_m-2\nu_m^2)]}$$

$$n=\frac{E_m^2 c_m(1+c_r-c_m\nu_m)+2c_m c_r(k_r n_r-l_r^2)(1+\nu_m)^2(1-2\nu_m)}{(1+\nu_m)[E_m(1+c_r-2\nu_m)+2c_m k_r(1-\nu_m-2\nu_m^2)]}+\frac{E_m[2c_m^2 k_r(1-\nu_m)+c_r n_r(1+c_r-2\nu_m)-4c_m l_r\nu_m]}{E_m(1+c_r-2\nu_m)+2c_m k_r(1-\nu_m-2\nu_m^2)} \tag{13}$$

$$p=\frac{E_m[E_m c_m+2p_r(1+\nu_m)(1+c_r)]}{2(1+\nu_m)[E_m(1+c_r)+2c_m p_r(1+\nu_m)]}$$

$$m=\frac{E_m[E_m c_m+2m_r(1+\nu_m)(3+c_r-4\nu_m)]}{2(1+\nu_m)\{E_m[c_m+4c_r(1-\nu_m)]+2c_m m_r(3-\nu_m-4\nu_m^2)\}}$$

where C_m and C_r are the volume fractions of the matrix and the CNTs respectively, and k_r ، l_r ، n_r ، p_r, m_r are the Hills elastic modulus for the CNTs [1]. The experimental results reveal that most of the CNTs are bent and centralized in one area of the polymer. These regions with concentrated CNTs are assumed in this section to have spherical shapes and are deliberated as "inclusions" with different elastic properties from the surrounding material. The total volume V_r of CNTs can be divided into the following two parts [1]:

$$V_r=V_r^{inclusion}+V_r^m \tag{14}$$

where $V_r^{inclusion}$ and V_r^m are the volumes of CNTs dispersed in the inclusions, concentrated regions, and in the matrix, respectively. Introduce two parameters ξ and ζ describe the agglomeration of CNTs:

$$\xi=\frac{V_{inclusion}}{V}, \tag{15}$$

$$\zeta=\frac{V_r^{inclusion}}{V_r}. \tag{16}$$

Despite that, the average volume fraction C_r of CNTs in the composite is:

$$C_r=\frac{V_r}{V}. \tag{17}$$

Assume that all the orientations of the CNTs are completely random. Hence, the effective bulk modulus (K) and effective shear modulus (G) may be written as:

$$K=K_{out}\left[1+\frac{\xi\left(\frac{K_{in}}{K_{out}}-1\right)}{1+\alpha(1-\xi)\left(\frac{K_{in}}{K_{out}}-1\right)}\right], \tag{18}$$

$$G=G_{out}\left[1+\frac{\xi\left(\frac{G_{in}}{G_{out}}-1\right)}{1+\beta(1-\xi)\left(\frac{G_{in}}{G_{out}}-1\right)}\right], \tag{19}$$

where:

$$K_{in}=K_m+\frac{(\delta_r-3K_m\chi_r)C_r\zeta}{3(\xi-C_r\zeta+C_r\zeta\chi_r)}, \tag{20}$$

$$K_{out}=K_m+\frac{C_r(\delta_r-3K_m\chi_r)(1-\zeta)}{3\left[1-\xi-C_r(1-\zeta)+C_r\chi_r(1-\zeta)\right]}, \tag{21}$$

$$G_{in}=G_m+\frac{(\eta_r-3G_m\beta_r)C_r\zeta}{2(\xi-C_r\zeta+C_r\zeta\beta_r)}, \tag{22}$$

$$G_{out}=G_m+\frac{C_r(\eta_r-3G_m\beta_r)(1-\zeta)}{2\left[1-\xi-C_r(1-\zeta)+C_r\beta_r(1-\zeta)\right]}, \tag{23}$$

where χ_r, β_r, δ_r, η_r may be calculated as:

$$\chi_r=\frac{3(K_m+G_m)+k_r-l_r}{3(k_r+G_m)}, \tag{24}$$

$$\beta_r=\frac{1}{5}\left\{\frac{4G_m+2k_r+l_r}{3(k_r+G_m)}+\frac{4G_m}{(p_r+G_m)}+\frac{2\left[G_m(3K_m+G_m)+G_m(3K_m+7G_m)\right]}{G_m(3K_m+G_m)+m_r(3K_m+7G_m)}\right\}, \tag{25}$$

$$\delta_r=\frac{1}{3}\left[n_r+2l_r+\frac{(2k_r-l_r)(3K_m+2G_m-l_r)}{k_r+G_m}\right], \tag{26}$$

$$\eta_r = \frac{1}{5}\left[\begin{array}{l} \frac{2}{3}(n_r - l_r) + \frac{4G_m p_r}{(p_r + G_m)} \\ + \frac{8G_m m_r (3K_m + 4G_m)}{3K_m (m_r + G_m) + G_m (7m_r + G_m)} \\ + \frac{2(k_r - l_r)(2G_m + l_r)}{3(k_r + G_m)} \end{array}\right]. \quad (27)$$

where K_m and G_m are the bulk and shear moduli of the matrix which can be written as:

$$K_m = \frac{E_m}{3(1-2\upsilon_m)} \quad (28)$$

$$G_m = \frac{E_m}{2(1+\upsilon_m)}. \quad (29)$$

Furthermore, β and α can be obtained from:

$$\alpha = \frac{(1+\upsilon_{out})}{3(1-\upsilon_{out})}, \quad (30)$$

$$\beta = \frac{2(4-5\upsilon_{out})}{15(1-\upsilon_{out})}, \quad (31)$$

$$\upsilon_{out} = \frac{3K_{out} - 2G_{out}}{6K_{out} + 2G_{out}}. \quad (32)$$

Finally, the elastic modulus (E) and Poisson's ratio (υ) can be computed as:

$$E = \frac{9KG}{3K+G}, \quad (33)$$

$$\upsilon = \frac{3K-2G}{6K+2G}. \quad (34)$$

2.6. Equations of Motion

The governing differential equations of motion are derived applying Hamilton's principle, which is given as [35]:

$$\int_0^T (\delta U + \delta V - \delta K)dt = 0 \quad (35)$$

where δU is the virtual strain energy which is obtained by the following relation [36]:

$$\delta U = \frac{1}{2}\iiint_V \left[\sigma_{ij}\varepsilon_{ij} - D_i E_i\right]dV \quad (36)$$

δK is the virtual kinetic energy and is defined as following [37]:

$$\delta K = \frac{1}{2}\iiint_V \left[(\dot{u})^2 + (\dot{v})^2 + (\dot{w})^2\right]dV \quad (37)$$

Also, δV is the virtual work operated by externally applied forces and is acquired by:

$$\delta U = \frac{1}{2}\iiint_V \left[q_e + q_m\right]dV \quad (38)$$

in which q_m can be written as:

$$q_m = \eta H_x^{\,2}\frac{\partial^2 w}{\partial x^2}, \quad (39)$$

where η is the magnetic permeability; ∇ is the gradient operator; H_x is the magnetic field. Furthermore, q_e can be written as:

$$q_e = k_w w - k_g \nabla^2 w, \quad (40)$$

where k_w and k_g are spring and shear constants of an elastic medium, respectively.

The motion equations can be derived by applying Eq. (35) as follows:

$$\begin{aligned} &\frac{\partial N_{xx}}{\partial x} + \frac{\partial N_{xy}}{\partial y} = m_0\frac{\partial^2 u_0}{\partial t^2}, \\ &\frac{\partial N_{xy}}{\partial x} + \frac{\partial N_{yy}}{\partial y} = m_0\frac{\partial^2 v_0}{\partial t^2}, \\ &\frac{\partial^2 M_{xx}}{\partial x^2} + 2\frac{\partial^2 M_{xy}}{\partial y \partial x} + \frac{\partial^2 M_{yy}}{\partial y^2} \\ &+ \frac{\partial}{\partial x}(N_{xx}\frac{\partial w_0}{\partial x} + N_{xy}\frac{\partial w_0}{\partial y}) \\ &+ \frac{\partial}{\partial y}(N_{xy}\frac{\partial w_0}{\partial x} + N_{yy}\frac{\partial w_0}{\partial y}) \\ &- K_W w_0 + K_G(\frac{\partial^2 w_0}{\partial x^2} + \frac{\partial^2 w_0}{\partial y^2}) \\ &+ q_e + q_m = m_0\frac{\partial^2 w_0}{\partial t^2} - m_2\frac{\partial^2}{\partial t^2}(\frac{\partial^2 w_0}{\partial x^2} + \frac{\partial^2 w_0}{\partial y^2}), \end{aligned} \quad (41)$$

where:

$$(m_0, m_2) = \int_{-h/2}^{h/2}\rho_0(1, z^2)dz \quad (42)$$

where (m_0, m_2) are mass moments of inertia, and ρ_0 denotes the density of the material. Meanwhile, the force resultants (N_{xx}, N_{yy}, N_{xy}) and the moment resultants (M_{xx}, M_{yy}, M_{xy}) of the plate can be defined as:

$$\left\{(N_x, N_y, N_{xy}), (M_x, M_y, M_{xy})\right\} = \int_{-h/2}^{h/2}\left\{\sigma_x, \sigma_y, \tau_{xy}\right\}(1, z)dz \quad (43)$$

Charge equation for coupling electrical and mechanical fields is:

$$\frac{\partial D_x}{\partial x} + \frac{\partial D_y}{\partial y} + D_z = 0, \quad (44)$$

In this study, transverse vibration is investigated (i.e., u_0=v_0=0).

3. DQ Method

As can be observed, the coupled governing equations contain nonlinear terms and should be solved applying a numerical method such as DQM. In this method, the differential equations are changed into a first-order algebraic equation by employing appropriate weighting coefficients. Weighting coefficients are not correlated to any special problem and only depend on the grid spacing. For the implementation of the DQ approximation, consider a function $f(\zeta, \eta)$ which has the field on a rectangular domain ($0 \le \zeta \le 1$ and $0 \le \eta \le 1$) with $n_\zeta \times n_\eta$ grid points along x and y axes. According to DQ method, the r^{th} derivative of a function $f(x, y)$ can be defined as [35]:

$$\left.\frac{\partial^r f(\zeta,\eta)}{\partial \zeta^r}\right|_{(\zeta,\eta)=(\zeta_i,\eta_j)} = \sum_{m=1}^{n_\zeta} C_{im}^{\zeta(r)} f(\zeta_m,\eta_j) = \sum_{m=1}^{n_x} C_{im}^{\zeta(r)} f_{mj}, \quad \begin{cases} i=1,2,...,n_\zeta \\ j=1,2,...,n_\eta \\ r=1,2,...,n_\zeta-1 \end{cases} \tag{45}$$

where C_{ij}^{ζ} are weighting coefficients and defined as:

$$C_{ij}^{\zeta} = \begin{cases} \dfrac{M(\zeta_i)}{(\zeta_i-\zeta_j)M(\zeta_j)} & for\ i \ne j \\ -\sum\limits_{\substack{j=1 \\ i\ne j}}^{n_\zeta} C_{ij}^{\zeta} & for\ i=j \end{cases}, \tag{46}$$

where $M(\zeta_i)$ is Lagrangian operators which can be presented as:

$$M(\zeta_i) = \prod_{\substack{j=1 \\ i\ne j}}^{n_\zeta} (\zeta_i - \zeta_j). \tag{47}$$

The weighting coefficients for the second, third, and fourth derivatives are defined as:

$$\begin{aligned} C_{ij}^{\zeta(2)} &= \sum_{k=1}^{n_\zeta} C_{ik}^{\zeta(1)} C_{kj}^{\zeta(1)}, \\ C_{ij}^{\zeta(3)} &= \sum_{k=1}^{n_\zeta} C_{ik}^{\zeta(1)} C_{kj}^{\zeta(2)} = \sum_{k=1}^{n_\zeta} C_{ik}^{\zeta(2)} C_{kj}^{\zeta(1)} \\ C_{ij}^{\zeta(4)} &= \sum_{k=1}^{n_\zeta} C_{ik}^{\zeta(1)} C_{kj}^{\zeta(3)} = \sum_{k=1}^{n_\zeta} C_{ik}^{\zeta(3)} C_{kj}^{\zeta(1)}. \end{aligned} \tag{48}$$

In a similar method, the weighting coefficients for y-direction can be acquired. The coordinates of grid points are chosen as:

$$\begin{aligned} \zeta_i &= \frac{1}{2}\left[1-\cos\left(\frac{\pi(i-1)}{(n_x-1)}\right)\right], \\ \eta_j &= \frac{1}{2}\left[1-\cos\left(\frac{\pi(j-1)}{(n_y-1)}\right)\right]. \end{aligned} \tag{49}$$

In order to carry out the eigenvalue analysis, the domain and boundary points are separated, and in vector forms, they are denoted as $\{d\}$ and $\{b\}$, respectively. Hence, the discretized form of the motion equations together with the boundary conditions can be expressed in matrix form as:

$$\left(\underbrace{\left[K_L + K_{NL}\right]}_{[K]} - \Omega^2 [M] \right) \begin{bmatrix} \{d\} \\ \{b\} \end{bmatrix} = 0, \tag{50}$$

in which $[M]$, $[K_L]$, and $[K_{NL}]$ are the mass matrix, linear stiffness matrix, and nonlinear stiffness matrix. This nonlinear equation can now be solved by applying a direct iterative process as follows:

- First, nonlinearity is ignored by taking $[K_{NL}]=0$ to solve the eigenvalue problem expressed in equation (50). This yields the linear eigenvalue (Ω_L) and associated eigenvector. The eigenvector is consequently scaled up so that the maximum transverse displacement of the microplate is equal to the maximum eigenvector, i.e., the given vibration amplitude W_{max}^*.
- Applying linear eigenvector $[K_{NL}]$ could be evaluated. The eigenvalue problem is then solved by substituting $[K_{NL}]$ into equation (50). This would give the nonlinear eigenvalue (Ω_L) and the new eigenvector.
- The new nonlinear eigenvector is scaled up again, and the above procedure is repeated iteratively until the frequency values from the two subsequent iterations 'r' and 'r+1' satisfy the prescribed convergence criteria [38] as:

$$\frac{\left|\omega^{r+1} - \omega^r\right|}{\omega^r} < \varepsilon_0 \tag{51}$$

where ε_0 is a small value number, and in the present analysis, it is taken to be 0.1%.

4. Numerical Results and Discussion

Mechanical, thermal, and electrical properties of PVDF matrix and CNT reinforcement are chosen from Ref. [9]. The final converged solution applying the numerical procedure above is illustrated as the influences of the elastic medium, nonlocal parameter, volume percent of CNT, CNTs agglomeration and temperature change on the frequency of the structure.

Since no reference to such a work is found to-date in the literature, its validation is not possible. Despite that, the present work could be partially validated based on a simplified analysis suggested by Shen et al. [14] on thermal nonlinear vibration

of the SLGS for which the coupled plate and volume percent of CNTs in the polymer were ignored. For this purpose, a SLGS with C_r=0, T=300 K, l=9.496 nm, b=4.877 nm, h=0.145 nm, ρ_0=5624 kg/m^3, k_w=k_g=0 and e_0a=0.67 nm is considered. Table 1 reveals the result of validation exercise by showing nonlinear-to-linear frequency for dissimilar dimensionless amplitude (w/h) and temperature. As it can be observed, the results acquired are in good agreement with those expressed in [14].

Fig. 2 manifests the effects of the nonlocal parameter on the frequency versus the orientation angle of CNTs.

As can be observed, the frequency of the system decreases with considering size effects. This is due to the fact that the contemplating of nonlocal parameter decreases the interaction force between microplate atoms, and that leads to a softer structure.

The effect of volume percent of CNTs on the frequency versus the orientation angle of CNTs is shown in Fig. 3. It is clear that the frequency increases with increasing the volume percent of CNTs, and the influence of volume percent of CNTs on the frequency become more prominent at the middle angle. It is because with increasing the volume percent of CNTs, the stiffness of structure increases.

Fig. 4 manifests agglomeration effects on the frequency versus orientation angle of CNTs. As can be seen, contemplating agglomeration effects leads to lower frequency since the stability of the system decreases.

Fig. 5 illustrates the influence of the thermal gradient (ΔT) on the frequency versus the orientation angle of CNTs. It is evident that an increase in temperature change does not considerable effect on the frequency.

Fig. 6 indicates the effect of temperature variations on the results. It is observed by increasing the temperature difference, the frequency enhances as a result to change in the mechanical properties of the structure.

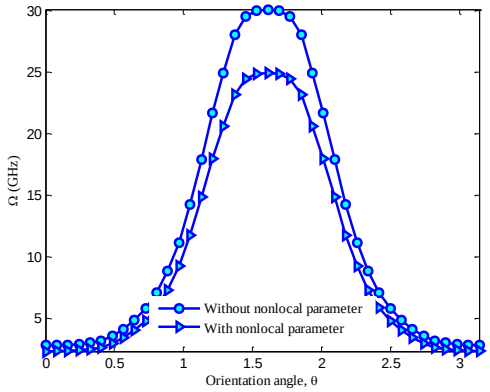

Fig. 2. The effects of the nonlocal parameter on the frequency versus the orientation angle of CNTs.

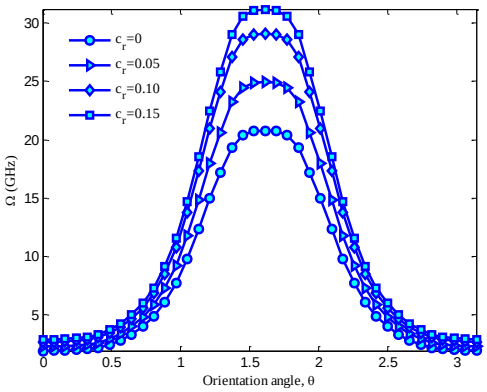

Fig. 3. The effects of volume percent of CNTs on the frequency versus the orientation angle of CNTs.

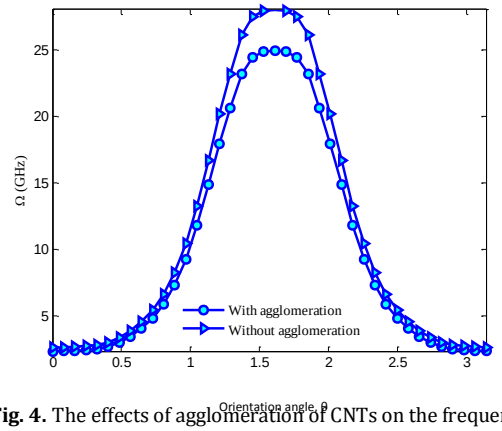

Fig. 4. The effects of agglomeration of CNTs on the frequency versus the orientation angle of CNTs.

Table 1. Comparing dimensionless nonlinear frequency obtained in the present study and those of Shen et al. [14].

Temperature	Ref.	Ω_{NL}/Ω_L			
		w/h=0.5	w/h=1	w/h=1.5	w/h=2
T=300 K	Present work	1.0208	1.0802	1.1742	1.2933
	Shen et al. [14]	1.0205	1.0798	1.1720	1.2900
	Difference (%)	0.029	0.037	0.188	0.256
T=400 K	Present work	1.0339	1.1292	1.2738	1.4492
	Shen et al. [14]	1.0337	1.1289	1.2719	1.4485
	Difference (%)	0.019	0.027	0.149	0.048
T=500 K	Present work	1.0731	1.2668	1.5372	1.8498
	Shen et al. [14]	1.0728	1.2663	1.5355	1.8477
	Difference (%)	0.028	0.039	0.111	0.114

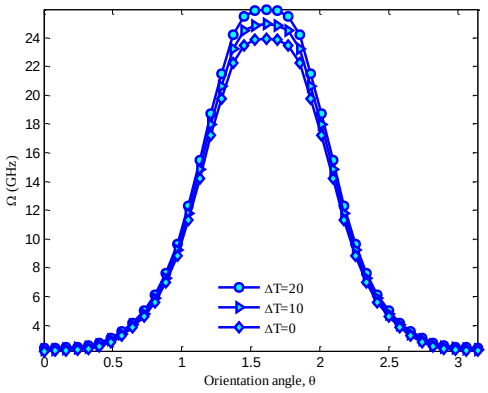

Fig. 5. The effects of thermal gradient on the frequency versus the orientation angle of CNTs.

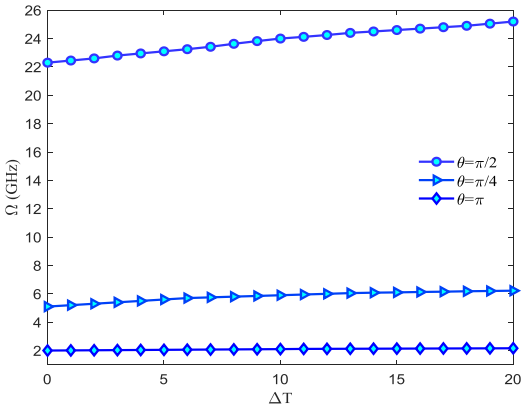

Fig. 6. The effects of temperature variations on the frequency.

The effect of elastic medium on the frequency of the structure is portrayed in Fig. 7. It can be found that considering elastic medium leads to higher frequency. Moreover, deliberating Pasternak medium predicts a higher frequency with respect to Winkler medium. It is due to the Pasternak medium, the normal and shear constant is taken into account.

The effect of foundation constants is discussed in Fig. 8. It can be observed that adding the spring to the structure, leads the frequency to increase and adding the shear layer, has a similar effect on the results as well.

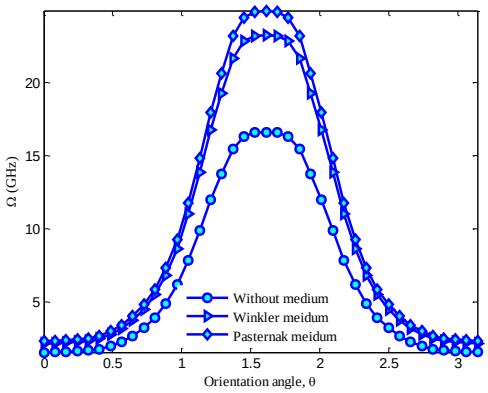

Fig. 7. The effects of the elastic medium on the frequency versus the orientation angle of CNTs.

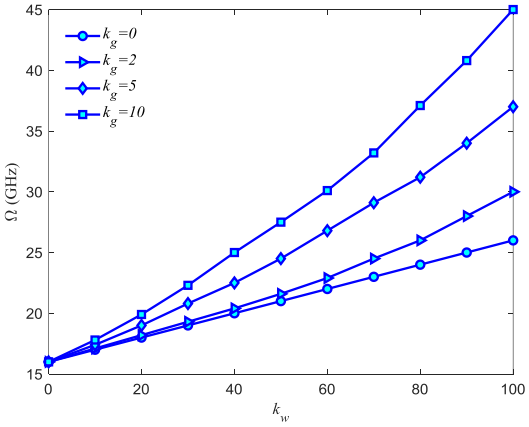

Fig. 8. The effects of foundation constants on the frequency.

The effect of the magnetic field on the frequency of structure is illustrated in Fig. 9. It can be found that increasing the magnetic field, the frequency increases. It is due to the increasing magnetic field leads to higher stiffness.

5. Conclusions

The vibration response of piezoelectric nano/micro composites has applications in designing many NEMS/MEMS devices such as hydraulic sensors and actuators. In the present study, electro-magneto nonlinear vibration of a double-piezoelectric composite microplate made of PVDF reinforced by CNTs is inspected deliberating agglomeration effects. The internal elastic medium between two microplates is simulated as Pasternak foundation. Considering charge equation, the nonlinear motion equations are derived based on nonlocal piezoelasticity theory. The DQM is applied in order to acquire the nonlinear frequency ratio of the DPCMPS so that the effects of the small scale coefficient, stiffness of the internal elastic medium, the volume fraction, and orientation angle of the CNTs reinforcement, temperature change and agglomeration are discussed.

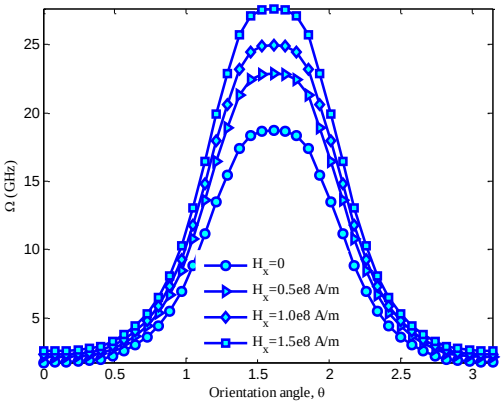

Fig. 9. The effects of the magnetic field on the frequency versus the orientation angle of CNTs.

The results of this study are validated by Shen et al. [14]. The results reveal that along with increasing geometrical aspect ratio, the effect of coupling elastic medium between two piezoelectric composite microplates decreases. Furthermore, the effects of small scale parameters and volume percent lead to a higher frequency. It is noteworthy to mention that the frequency of structure considering the agglomeration of CNTs becomes lower.

Acknowledgment

The authors would like to thank the reviewers for their valuable comments and suggestions to improve the clarity of this study.

Funding

The authors are thankful to the University of Kashan for supporting this work by Grant No. 891255/2.

References

[1] Pissis P. Thermoset nanocomposites for engineering applications: iSmithers Rapra Publishing; 2007.
[2] Merhari L. Hybrid nanocomposites for nanotechnology: Springer; 2009.
[3] Schwartz M. Encyclopedia of Smart Materials, 2 Volume Set. *Encyclopedia of Smart Materials, 2 Volume Set, by Mel Schwartz, pp 1176 ISBN 0-471-17780-6 Wiley-VCH, March 2002* 2002: 1176.
[4] Topolov VY, Bowen CR. Electromechanical properties in composites based on ferroelectrics: Springer Science & Business Media; 2008.
[5] Yang J. The mechanics of piezoelectric structures: World Scientific; 2006.
[6] Brockmann TH. Theory of Adaptive Fiber Composites: from piezoelectric material behavior to dynamics of rotating structures: Springer Science & Business Media; 2009.
[7] Arnau A. Piezoelectric transducers and applications: Springer; 2004.
[8] Barzoki AM, Arani AG, Kolahchi R, Mozdianfard M. Electro-thermo-mechanical torsional buckling of a piezoelectric polymeric cylindrical shell reinforced by DWBNNTs with an elastic core. *Applied Mathematical Modelling* 2012; 36(7): 2983-95.
[9] Barzoki AM, Arani AG, Kolahchi R, Mozdianfard M, Loghman A. Nonlinear buckling response of embedded piezoelectric cylindrical shell reinforced with BNNT under electro–thermo-mechanical loadings using HDQM. *Composites Part B: Engineering* 2013; 44(1): 722-7.
[10] Arani AG, Shajari A, Amir S, Loghman A. Electro-thermo-mechanical nonlinear nonlocal vibration and instability of embedded micro-tube reinforced by BNNT, conveying fluid. *Physica E: Low-dimensional Systems and Nanostructures* 2012; 45: 109-21.
[11] Eringen AC. Nonlocal polar elastic continua. *International journal of engineering science* 1972; 10(1): 1-16.
[12] Eringen AC. On differential equations of nonlocal elasticity and solutions of screw dislocation and surface waves. *Journal of applied physics* 1983; 54(9): 4703-10.
[13] Eringen AC. Nonlocal continuum field theories: Springer Science & Business Media; 2002.
[14] Shen L, Shen H-S, Zhang C-L. Nonlocal plate model for nonlinear vibration of single layer graphene sheets in thermal environments. *Computational Materials Science* 2010; 48(3): 680-5.
[15] Pradhan S, Kumar A. Vibration analysis of orthotropic graphene sheets embedded in Pasternak elastic medium using nonlocal elasticity theory and differential quadrature method. *Computational Materials Science* 2010; 50(1): 239-45.
[16] Amir S. Orthotropic patterns of visco-Pasternak foundation in nonlocal vibration of orthotropic graphene sheet under thermo-magnetic fields based on new first-order shear deformation theory. *Proceedings of the Institution of Mechanical Engineers, Part L: Journal of Materials: Design and Applications* 2019; 233(2): 197-208.
[17] Arani AG, Barzoki AM, Kolahchi R, Loghman A. Pasternak foundation effect on the axial and torsional waves propagation in embedded DWCNTs using nonlocal elasticity cylindrical shell theory. *Journal of mechanical science and technology* 2011; 25(9): 2385.
[18] Zhou Z-G, Wang B. The scattering of harmonic elastic anti-plane shear waves by a Griffith crack in a piezoelectric material plane by using the non-local theory. *International Journal of Engineering Science* 2002; 40(3): 303-17.
[19] Zhou Z-G, Wu L-Z, Du S-Y. Non-local theory solution for a Mode I crack in piezoelectric materials. *European Journal of Mechanics-A/Solids* 2006; 25(5): 793-807.
[20] Zhou Z-G, Du S-Y, Wu L-Z. Investigation of anti-plane shear behavior of a Griffith permeable crack in functionally graded piezoelectric materials by use of the non-local theory. *Composite structures* 2007; 78(4): 575-83.
[21] Ke L-L, Wang Y-S, Wang Z-D. Nonlinear vibration of the piezoelectric nanobeams based on the nonlocal theory. *Composite Structures* 2012; 94(6): 2038-47.

[22] Sobhy M, Zenkour AM. Magnetic field effect on thermomechanical buckling and vibration of viscoelastic sandwich nanobeams with CNT reinforced face sheets on a viscoelastic substrate. *Composites Part B: Engineering* 2018; 154: 492-506.
[23] Arani AG, Jamali S, Zarei HB. Differential quadrature method for vibration analysis of electro-rheological sandwich plate with CNT reinforced nanocomposite facesheets subjected to electric field. *Composite Structures* 2017; 180: 211-20.
[24] Tohidi H, Hosseini-Hashemi S, Maghsoudpour A. Nonlinear size-dependent dynamic buckling analysis of embedded micro cylindrical shells reinforced with agglomerated CNTs using strain gradient theory. *Microsystem Technologies* 2017; 23(12): 5727-44.
[25] Murmu T, Adhikari S. Nonlocal vibration of bonded double-nanoplate-systems. *Composites Part B: Engineering* 2011; 42(7): 1901-11.
[26] Murmu T, Sienz J, Adhikari S, Arnold C. Nonlocal buckling behavior of bonded double-nanoplate-systems. *Journal of Applied Physics* 2011; 110(8): 084316.
[27] Pouresmaeeli S, Fazelzadeh S, Ghavanloo E. Exact solution for nonlocal vibration of double-orthotropic nanoplates embedded in elastic medium. *Composites Part B: Engineering* 2012; 43(8): 3384-90.
[28] Arani AG, Shiravand A, Rahi M, Kolahchi R. Nonlocal vibration of coupled DLGS systems embedded on Visco-Pasternak foundation. *Physica B: Condensed Matter* 2012; 407(21): 4123-31.
[29] Arani AG, Kolahchi R, Vossough H. Buckling analysis and smart control of SLGS using elastically coupled PVDF nanoplate based on the nonlocal Mindlin plate theory. *Physica B: Condensed Matter* 2012; 407(22): 4458-65.
[30] Amir S, Bidgoli EM-R, Arshid E. Size-dependent vibration analysis of a three-layered porous rectangular nano plate with piezo-electromagnetic face sheets subjected to pre loads based on SSDT. *Mechanics of Advanced Materials and Structures* 2018: 1-15.
[31] Reddy JN. Mechanics of laminated composite plates and shells: theory and analysis: CRC press; 2004.
[32] Vinson JR. Plate and panel structures of isotropic, composite and piezoelectric materials, including sandwich construction: Springer Science & Business Media; 2006.
[33] Tan P, Tong L. Micro-electromechanics models for piezoelectric-fiber-reinforced composite materials. *Composites science and technology* 2001; 61(5): 759-69.
[34] Arshid E, Kiani A, Amir S. Magneto-electro-elastic vibration of moderately thick FG annular plates subjected to multi physical loads in thermal environment using GDQ method by considering neutral surface. *Proceedings of the Institution of Mechanical Engineers, Part L: Journal of Materials: Design and Applications* 2019: 1464420719832626.
[35] Arshid E, Khorshidvand AR. Free vibration analysis of saturated porous FG circular plates integrated with piezoelectric actuators via differential quadrature method. *Thin-Walled Structures* 2018; 125: 220-33.
[36] Arshid E, Khorshidvand AR, Khorsandijou SM. The effect of porosity on free vibration of SPFG circular plates resting on visco-Pasternak elastic foundation based on CPT, FSDT and TSDT. *Structural Engineering and Mechanics* 2019; 70(1): 97-112.
[37] Arshid E, Khorshidvand AR. Flexural Vibrations analysis of saturated porous circular plates using differential quadrature method. *Iranian Journal of Mechanical Engineers* 2017; 19: 78-100.
[38] Arani AG, Kolahchi R, Barzoki AAM, Mozdianfard MR, Farahani SMN. Elastic foundation effect on nonlinear thermo-vibration of embedded double-layered orthotropic graphene sheets using differential quadrature method. *Proceedings of the Institution of Mechanical Engineers, Part C: Journal of Mechanical Engineering Science* 2013; 227(4): 862-79.